TRANSITION METAL CHEMISTRY

A Series of Advances

EDITED BY

RICHARD L. CARLIN

DEPARTMENT OF CHEMISTRY
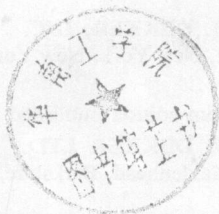UNIVERSITY OF ILLINOIS AT CHICAGO CIRCLE
CHICAGO, ILLINOIS

VOLUME 5

1969

MARCEL DEKKER New York and London

TRANSITION METAL CHEMISTRY

Volume 5

Contributors to Volume 5

Leslie S. Forster, *Department of Chemistry, University of Arizona, Tucson, Arizona*

Gilbert Gordon, *Department of Chemistry, University of Iowa, Iowa City, Iowa*

William E. Hatfield, *Department of Chemistry, University of North Carolina, Chapel Hill, North Carolina*

Gerald F. Kokoszka, *National Bureau of Standards, Washington, D.C., and State University of New York, College at Plattsburgh, Plattsburgh, New York*

Robin Whyman,* *Department of Chemistry, University of North Carolina, Chapel Hill, North Carolina*

* Present address: Imperial Chemical Industries, Ltd., Petrochemical and Polymer Laboratory, Runcorn, Cheshire, England.

v

Contents of Other Volumes

OTHER VOLUMES

To be announced

Contents of Volume 5

The Spectra of Chromium(III) Complexes 1

Leslie S. Forster

Copper Complexes 47

William E. Hatfield and Robin Whyman

Metal–Metal Exchange Interactions   **181**

Gerald F. Kokoszka and Gilbert Gordon

THE SPECTRA OF
CHROMIUM(III) COMPLEXES

LESLIE S. FORSTER

DEPARTMENT OF CHEMISTRY
UNIVERSITY OF ARIZONA
TUCSON, ARIZONA

I. INTRODUCTION

The spectra of the transition metal ions as a class have been reviewed many times (1–5), but in this survey attention is focused upon the electronic spectra of one species, Cr(III). Interest in Cr(III) spectroscopy may be traced back to E. Becquerel, who reported the luminescence lifetime of ruby in 1867, and there now exists an immense body of experimental and theoretical work dealing with this species. An upsurge of activity has been occasioned by the development of the ruby laser, and the field of Cr(III) spectroscopy is now heavily populated by both chemists and physicists.

A survey of Cr(III) spectroscopy is propitious for several reasons. The accumulation of a vast literature is sufficient justification in itself. More-over, the variety of available experimental information permits a critical evaluation of existing theory.

1

Both theory and experiment may be characterized in terms of resolution. Even as spectral details can be recorded at low and high resolution, so can one employ low- and high-resolution theory. Thus ligand field theory, in which noncubic distortions and spin-orbit coupling are neglected, is a low-resolution theory. The inclusion of axial fields and spin-orbit coupling increases the theoretical resolution in the same way that reduction of the temperature and narrowing of the spectrograph slit often reveals details otherwise obscured. In this review both theory and experiment will be treated, progressively, at increasing resolution.

It is a useful approximation to categorize transitions in the spectra of transition metal ions as (1) metal-localized, (2) ligand-localized, and (3) charge-transfer transitions. The emphasis here will be upon the metal-localized (d-d) transitions, and only brief reference to the other two categories will be made.

It is convenient to classify Cr(III) systems as ionic or molecular. Ruby ($Cr^{3+}: Al_2O_3$) is a good example of an ionic system, while molecular complexes can be charged [$Cr(NH_3)_6^{3+}$] or uncharged [$Cr(acac)_3$]. A molecular complex can be considered as a well-defined species whose identity is the same in the liquid or solid state, whereas the properties of an ionic complex are intimately related to those of the crystal lattice. Ionic crystals are sometimes termed "hard," while molecular crystals are called "soft."

When a free Cr(III) ion is incorporated into a complex, both the energies and intensities of the electronic transitions are altered profoundly. In addition, nonradiative pathways for the dissipation of excitation energy are introduced. In this review we will be primarily concerned with the effect of environment upon the energies and probabilities (radiative and nonradiative) of electronic transitions. Although the literature has been surveyed through the end of 1967, no attempt at encyclopedic coverage has been made.

II. ENERGY LEVELS

With very few exceptions (6,7), Cr(III) is hexacoordinated; the nearest-neighbor atoms are arranged in an octahedral or nearly octahedral array. Two quartet states, ^4F and ^4P, and five doublet states, ^2P, ^2G, ^2D, ^2H, and ^2F, are derived from the d^3 configuration. In an octahedral ligand field, ^4F is split into the $^4A_2$, $^4T_1$, and $^4T_2$ states. The only other ligand field states that have been observed in Cr(III) spectra are $^4T_1(^4P)$ and ^2E, $^2T_1$, and $^2T_2$ derived from ^2G.

A complete ligand field calculation has been made by Liehr (8) and a simplified version of his results is presented in Fig. 1. The three expected spin-allowed *d-d* transitions,

$$^4T_2 \leftarrow {}^4A_2, \qquad {}^4T_1(^4F) \leftarrow {}^4A_2, \qquad {}^4T_1(^4P) \leftarrow {}^4A_2$$

are observed in the spectrum of ruby (Fig. 2).

In this section, effects due to spin-orbit coupling and deviations from O_h symmetry will be neglected. In this approximation, ligand field theory requires the evaluation of two parameters for the assignment of the
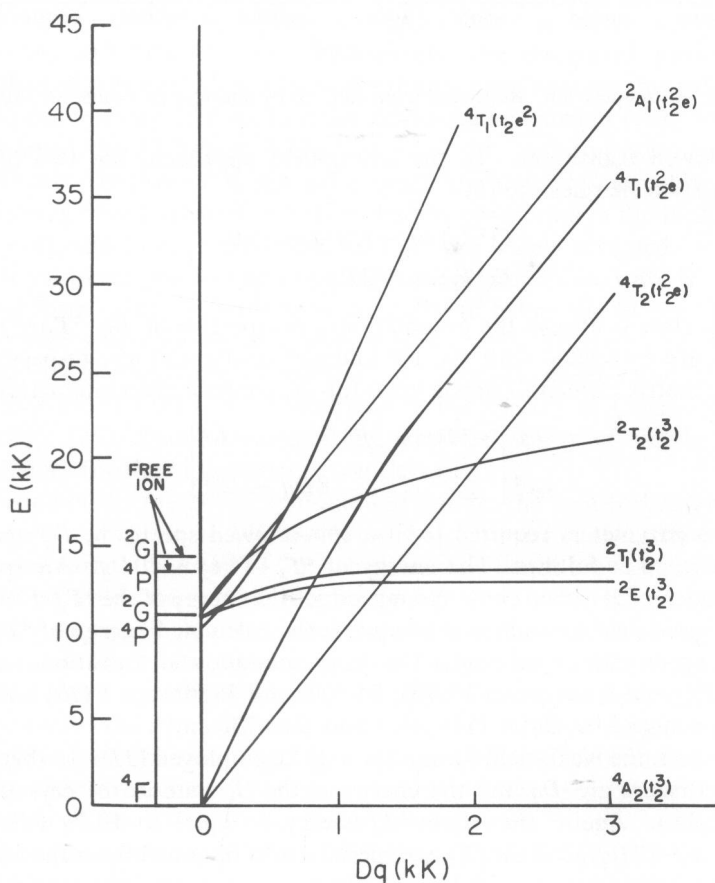
Fig. 1. Calculated Cr^{3+} energy levels. Parameters: $B = 680\ cm^{-1}$, $C = 4B$, $\zeta = 175\ cm^{-1}$. [After Liehr (8).]
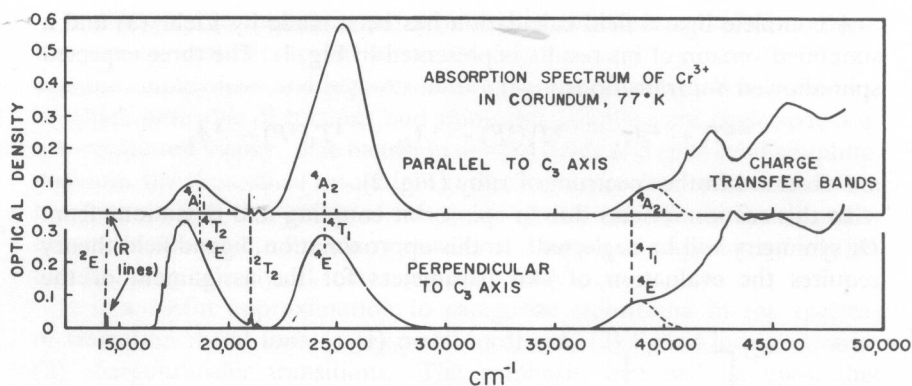
Fig. 2. Ruby spectrum. Reprinted from Ref. (3) by courtesy of Academic Press.

spin-allowed transitions. In the strong-field approach, the two lowest quartet state energies are (9)

$$E(^4A_2) = -12Dq - 15B$$
$$E(^4T_2) = -2Dq - 15B$$

The $^4A_2$ state is always the ground state, irrespective of Dq. $^4T_1(^4F)$ and $^4T_1(^4P)$ are correlated with the t_2^2e and t_2e^2 configurations, respectively, and the matrix elements (strong field) for the configuration interaction are

$$\begin{array}{c} t_2^2e \\ t_2e^2 \end{array} \begin{vmatrix} -2Dq - 3B & 6B \\ & 8Dq - 12B \end{vmatrix}$$

The two parameters required to fit a spin-allowed spectrum, Dq and B, are evaluated as follows. The energy of $^4T_2 \leftarrow {}^4A_2$ is $10Dq$. An appropriate value of B is then chosen to reproduce the energy of the $^4T_1(^4F)$ state. If the ligand field formalism is adequate, the calculated energy of $^4T_1(^4P)$ should agree with experiment. The three spin-allowed transitions in the $Cr(H_2O)_6^{3+}$ spectrum are at 17,400, 24,500, and 38,000 cm^{-1} (10) and are well reproduced by $Dq = 1740$ cm^{-1} and $B = 730$ cm^{-1}.

If desired, the weak-field formalism may be employed (11). In this case the parameters are Dq and the energy of the ^4P state in the crystal (cf. Section IV). Again, the $^4T_2 \leftarrow {}^4A_2$ energy is equal to $10Dq$ (the $^4A_2$ energy is $-12Dq$), but the $^4T_1$ energies are now obtained from the matrix (12)

$$\begin{array}{c} ^4T_1(^4F) \\ ^4T_1(^4P) \end{array} \begin{vmatrix} 6Dq & 4Dq \\ & E(^4P) \end{vmatrix}$$

and a good spectral fit is obtained with $Dq = 1740$ cm^{-1} and $E(^4P) = 10,400$ cm^{-1}.

The $^4T_1(^4P) \leftarrow {}^4A_2$ transition is often obscured by charge-transfer or ligand transitions and the adequacy of the simple ligand field model has been tested in only a few instances. In addition to the $Cr(H_2O)_6^{3+}$ spectrum, the spectra of K_2NaCrF_6 (13), emerald (13), and ruby (3) are well reproduced by two parameters.

That ligand field theory is not always completely satisfactory is well illustrated by the example of Cr^{3+}:MgO. The absorption spectrum of Cr^{3+}:MgO consists of three broad strong bands at 16,200, 22,700, and 29,700 cm^{-1} (12). If the 16,200- and 22,700-cm^{-1} bands are assigned as $^4T_2 \leftarrow {}^4A_2$ and $^4T_1(^4F) \leftarrow {}^4A_2$, respectively, the computed position of $^4T_1(^4P)$ is 36,000 cm^{-1}. The 6000-cm^{-1} discrepancy between this value and 29,700 cm^{-1} prompted Low to reject the above assignment (12). Instead, he assigned the 22,700-cm^{-1} band as $^4T_2 \leftarrow {}^4A_2$ and suggested that the 16,200-cm^{-1} transition might arise from an impurity, possibly Cr^{2+}. However, Cr^{3+} phosphorescence is excited by absorption in the 16,200-cm^1 band (14), and Low's assignment has not been widely accepted.

It is unreasonable to expect configuration interaction with $^4T_1$ states derived from other configurations, e.g., d^2s, to better the fit for $^4T_1(^4P)$, since these states lie at very high energies (15). Inclusion of charge-transfer states could improve matters. Schäffer also experienced difficulty in fitting the $^4T_1(^4P) \leftarrow {}^4A_2$ transitions in the spectra of $Cr(urea)_6^{3+}$ and $Cr(mal)_3^{3-}$ (16), again demonstrating the unreliability of simple ligand field theory for the higher-energy transitions.

In contrast to the broad spin-allowed bands, the spin-forbidden transitions, $^2E \leftarrow {}^4A_2$, $^2T_1 \leftarrow {}^4A_2$, and $^2T_2 \leftarrow {}^4A_2$, give rise to sharp lines which can be as narrow as 1 cm^{-1} (17). These narrow bands are associated with transitions within the same configuration, t_2^3. In this case the ground- and excited-state equilibrium geometries are nearly the same, and few vibrations are excited. Parenthetically, the energies of intraconfigurational spin-forbidden transitions are not very dependent upon Dq (18). On the other hand, the spin-allowed transitions are always associated with configurational changes, e.g., $t_2^3 \rightarrow t_2^2e$, and the noncoincidence of the ground- and excited-state potential surface minima (Fig. 3) leads to the excitation of many vibrations. Broad bands are the result. According to the above argument, a spin-forbidden transition such as $^2A_1 \leftarrow {}^4A_2$ would also be broad and likely to be obscured by the more intense spin-allowed bands. This would account for the observation of only three spin-forbidden transitions.

In the strong-field limit, ^2E and $^2T_1$ are degenerate, but configuration interaction removes this degeneracy in intermediate fields. The Liehr calculation for $Cr^{3+}:MgO$ predicts a splitting of about 700 cm^{-1}, with ^2E the lower (8). This calculated splitting is not too sensitive to the parameter values (19). The $^2E - ^2T_1$ splitting as computed for ruby
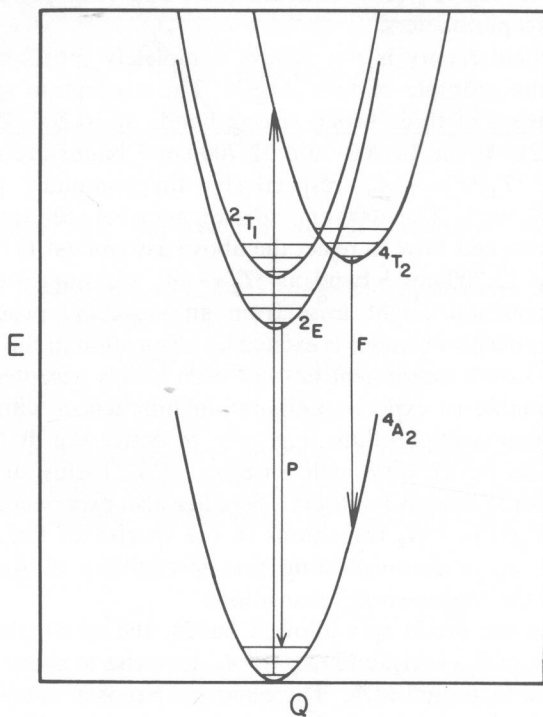
Fig. 3. Potential surfaces (schematic).

is also 700 cm^{-1} (20), in agreement with the observations in which the predicted order of the states is confirmed (21). The $^2E \rightarrow ^4A_2$ transition is of special interest because it is involved in the operation of the ruby laser. The lines produced by this transition are termed R lines. In MgO, where Cr^{3+} replaces Mg^{2+} substitutionally, most Cr^{3+} ions are in O_h sites and the single R line occurs at 6981 Å. In lower symmetries, two lines (R_1 and R_2) are observed. Associated with the R lines is vibronic structure (Section III.C).

Nearly all Cr(III) complexes luminesce ($^2E \rightarrow ^4A_2$), although low

temperatures are often required to obtain reasonable intensities, and the ^2E state can be located readily in both absorption and emission. The state energies of $^2T_1$ and $^2T_2$ cannot be evaluated so easily. These states

Table 1

ENERGIES (kK) AND NEPHELAUXETIC PARAMETERS FOR Cr(III) COMPLEXES

Complex	$^4T_2$	$^4T_1$	Ref.	^2E	Ref.	β_{35}^a	β_{55}^b	$\epsilon = 1 - \dfrac{B_{35}}{B_{55}}$
Cr^3:MgO	16.2	22.7	(12)	14.3	(31)	0.69	0.81	0.15
Cr^{3+}:Al$_2$O$_3$	18.1	24.4	(1)	14.4	(32)	0.66	0.81	0.19
Cr^{3+}:beryl	16.2	23.8	(13)	14.7	(13)	0.88	0.83	<0
CrF$_6^{3-}$ (K$_2$NaCrF$_6$)	15.9	23.2	(13)	15.2	(13)	0.92	0.86	<0
CrF$_6^{3-}$ (CrF$_3$)	14.9	22.7	(25)	15.7	(25)	0.97	0.89	<0
Cr(NH$_3$)$_6^{3+}$	21.5	28.9	(26)	15.1	(33)	0.77	0.84	0.08
Cr(H$_2$O)$_6^{3+}$	17.4	24.6	(26)	14.7	(34)	0.79	0.83	0.05
Cr(urea)$_6^{3+}$	16.1	22.6	(27)	14.2	(33)	0.71	0.80	0.11
Cr(CN)$_6^{3-}$	26.7	32.2	(25)	12.5	(35)	0.53	0.69	0.23
Cr(NCS)$_6^{3-}$	17.8	23.8	(1)	12.9	(33)	0.62	0.72	0.14
Cr(NH$_3$)$_5$H$_2$O^{3+}	20.8	27.8	(1)	15.0	(34)	0.72	0.84	0.14
Cr(NH$_3$)$_5$Cl^{2+}	19.4	26.6	(1)	14.8	(34)	0.77	0.83	0.07
Cr(NH$_3$)$_5$Br^{2+}	19.1	26.5	(1)	14.8	(34)	0.80	0.83	0.04
trans-Cr(NH$_3$)$_2$-(NCS)$_4^-$	19.4	25.6	(28)	13.3	(34)	0.64	0.74	0.14
Cr(ox)$_3^{3-}$	17.5	23.9	(26)	14.4	(33)	0.68	0.81	0.16
Cr(en)$_3^{3+}$	21.9	28.5	(26)	15.0	(33)	0.67	0.83	0.19
Cr(acac)$_3$	17.9	26.3(?)	(29)	12.9	(33)	0.98(?)	0.72	<0(?)
Cr(dtp)$_3$	14.3	18.9	(25)	11.0	(36)	0.44	0.62	0.29
cis-Cr(en)$_2$Cl$_2^+$	18.8	25.0	(30)	14.5	(34)	0.64	0.81	0.21
Cr(en)(ox)$_2^-$	18.8	25.4	(1)	14.4	(33)	0.69	0.81	0.15
Cr(en)$_2$(ox)$^+$	20.2	27.1	(1)	14.5	(33)	0.75	0.84	0.11
cis-Cr(en)$_2$(H$_2$O)$_2^{3+}$	20.6	27.3	(26)	15.1	(26)	0.78	0.84	0.07

[a] B obtained by fitting $^4T_2 - {^4T_1}$ (^4F) separation to the strong-field matrices (including CI).

[b] B computed from $2E$ energy (strong-field CI matrix). $\beta = B/B_0(B_0 = 920$ cm^{-1}).

must be observed in absorption and thick solid samples, or very concentrated solutions are required to detect the $^2T_1 \leftarrow {^4A_2}$ and $^2T_2 \leftarrow {^4A_2}$ transitions. In addition, these transitions are often obscured by the spin-allowed bands, but in a number of complexes these transitions have been identified (13,22,23).

The positions of the spin-allowed and spin-forbidden transitions are listed in Table 1. The effect of crystal structure is evidenced by the

100-cm^{-1} difference in Dq for CrF$_6^{3-}$ in two different lattices. A larger difference is noted when CrCl$_6^{3-}$ is present in CrCl$_3$ (13) and a molten salt solution (24).

The strong-field treatment of the spin-forbidden transitions requires three parameters, Dq and two Racah parameters (B and C). It is impoitant to recognize that the value of B obtained from fitting the spin-allowed bands is not usually applicable to the treatment of the spin-forbidden transitions. This problem is discussed in detail in Section IV.

III. INTENSITIES

A. Spin-Allowed Transitions

The transition energies of most Cr(III) complexes can be treated reasonably well in terms of an O_h model. Thus the spectra of Cr(ox)$_3^{3-}$, where the symmetry about the Cr^{3+} ion is D_3, and Cr(H$_2$O)$_6^{3+}$ can both be readily interpreted in O_h. It is only when the finer details of the spectrum are of interest that the true site symmetry need be considered. On the contrary, the intensities of d-d transitions can be very sensitive to the precise arrangement of the ligands about the central ion. This situation is not merely a reflection of the general quantum-mechanical principle that a first-order change in a wave function produces only a second-order change in the energy, but is intimately related to the mechanism by which the intensity is derived.

In the Born–Oppenheimer approximation, the total wave function is expressed as a product of electronic and vibrational parts,

$$\Psi_{i\mu} = \Theta_i(q, Q)\phi_\mu^i(Q) \tag{1}$$

where the electronic function depends upon both the electronic coordinates, q, and the nuclear coordinates, Q, while the vibrational function is only dependent upon nuclear positions. In an electronic transition, changes in both electronic and vibrational quantum numbers may occur (vibronic transition), $\Psi_{j\nu} \leftarrow \Psi_{i\mu}$. In the special case where $\nu = \mu = 0$, the transition $\Psi_{j0} \leftarrow \Psi_{i0}$ is termed the 0-0 transition, or the electronic origin. In the parlance of solid-state physics, the 0-0 transition is the no-phonon transition.

Transitions can be induced by the electric and magnetic components of electromagnetic radiation. The intensity of a given vibronic transition is proportional to $\langle \Psi_{j\nu}| \mu_e |\Psi_{i\mu}\rangle^2$ or $\langle \Psi_{j\nu}| \mu_m |\Psi_{i\mu}\rangle^2$ for electric and magnetic dipole transitions, respectively. The selection rules are determined from